

Article

Energetic and Spectroscopic Properties of the Low-Lying Isomers of C₅H: A High-Level Ab Initio Study

Sayon Satpati ^{1,†}, Tarun Roy ^{1,†}, Anakuthil Anoop ², Venkatesan S. Thimmakondur ^{3,*}
and Subhas Ghosal ^{1,*}

¹ Department of Chemistry, National Institute of Technology Durgapur, M G Avenue, Durgapur 713209, West Bengal, India

² Department of Chemistry, Indian Institute of Technology Kharagpur, Kharagpur 721302, West Bengal, India

³ Department of Chemistry and Biochemistry, San Diego State University, San Diego, CA 92182-1030, USA

* Correspondence: vthimmakondusamy@sdsu.edu (V.S.T.); subhas.ghosal@ch.nitdgp.ac.in (S.G.)

† These authors contributed equally to this work.

Abstract: Fourteen highly reactive isomers of C₅H and their ionic counterparts have been theoretically investigated using density functional theory (DFT) and coupled-cluster methods. The linear C₅H (*l*-C₅H) radical, pent-1,3-diyne-5-ylidene-1-yl (**1**), along with its cationic form and the cyclic C₅H (*c*-C₅H), 1-ethynylcycloprop-1-en-2-yl-3-ylidene (**2**), have recently been detected in the Taurus Molecular Cloud-1. By using the UCCSD(T)/cc-pCVTZ level of theory, the calculated rotational constants and other spectroscopic parameters are found to be in good agreement with the available experimental data for isomers **1** and **2**. Therefore, the current theoretical study may assist synthetic chemists and molecular spectroscopists in detecting other isomers in the laboratory or in the interstellar medium (ISM). Thermodynamically favorable rearrangement schemes for forming low-lying isomers **1**, **2**, and **3** have also been studied theoretically, and (2λ³-cycloprop-2-en-1-ylidene)ethenylidene (**3**) with a large dipole moment ($\mu = 4.73$ Debye) is proposed to be a plausible candidate for detection in the ISM.

Keywords: C₅H; DFT; coupled-cluster; ISM; rotational constant



check for updates

Citation: Satpati, S.; Roy, T.; Anoop, A.; Thimmakondur, V.S.; Ghosal, S. Energetic and Spectroscopic Properties of the Low-Lying Isomers of C₅H: A High-Level Ab Initio Study. *Atoms* **2023**, *11*, 115. <https://doi.org/10.3390/atoms11090115>

Academic Editor: Yew Kam Ho

Received: 30 June 2023

Revised: 21 August 2023

Accepted: 22 August 2023

Published: 24 August 2023



Copyright: © 2023 by the authors. Licensee MDPI, Basel, Switzerland. This article is an open access article distributed under the terms and conditions of the Creative Commons Attribution (CC BY) license (<https://creativecommons.org/licenses/by/4.0/>).

1. Introduction

Since the discovery of CH and CH⁺ molecules in the early 1940s [1–4], over 250 neutral, radical, ionic, and carbene molecules have been detected in the harsh environment of cold diffuse molecular clouds, dense star-forming regions, photodissociation, and circumstellar envelopes [5–7]. Out of all the molecules detected, approximately one-fourth of them are hydrocarbons, mostly unsaturated in nature, with a low H/C ratio [8]. These unsaturated hydrocarbons have not only played crucial roles in the chemical evolution of molecular gas clouds but also helped in the combustion processes and formation of polycyclic aromatic hydrocarbons (PAHs) through various resonantly stabilized free radicals (RSFRs) [9] and carbenes [10–12]. Many RSFRs have been identified as responsible carriers of unidentified diffuse interstellar bands (DIBs) [13].

The C_nH (n = 2 to 8) family of hydrocarbon radicals are the most important RSFRs detected in the interstellar medium (ISM) [8,14,15]. The low-molecular-weight RSFRs of C_nH with n = 2–4 have been detected in the star-forming and photo-dominated regions, translucent molecular clouds, circumstellar envelopes, and the diffuse medium [16–22], whereas the larger ones (with n = 5–8) are detected in the cold, dense molecular clouds and in the expanding envelope of the carbon-rich star, e.g., IRC+10216 [23–29]. Interestingly, the C_nH radicals with an even number of carbon atoms ('even') can be generated by the detachment of a hydrogen atom from a stable acetylenic chain, which can be described by standard valence bond structure. However,

C_nH radicals with an odd number of carbon atoms ('odd') have no such standard structure and cannot be formed from the closed-shell molecules. Thereby, 'odd' radicals are expected to be more reactive than the 'even' radicals [25,30]; therefore, they are less abundant in the ISM. However, the widespread detection of cyclic (*c*-) and linear (*l*-) forms of C_3H radicals, cyclopropan-1,2-diyliden-3-yl and prop-1-yn-3-ylidyne, in the ISM have opened up possibilities of identifying more numbers of RSFRs of C_nH family with an odd number of carbon atoms [20,22,25,30–35].

Linear C_5H isomer, pent-1,3-diyn-5-yliden-1-yl (**1**), was astronomically discovered by Cernicharo et al. in 1986 [25,26]. In the same year, Gottlieb and co-workers also identified the same molecule in the laboratory by employing microwave spectroscopy [36]. In 1999, McCarthy et al. successfully characterized *l*- C_5H [37]. The *c*- C_5H isomer, 1-ethynylcycloprop-1-en-2-yl-3-ylidene (**2**), was detected later in 2001 by Apponi et al. in a supersonic molecular beam experiment by Fourier transform microwave spectroscopy [38]. The linear isomeric form of the C_5H radical is more stable than the cyclic one [39], which is in contrast to the C_3H radical, where the cyclic isomer is more stable compared to the linear one. Interestingly, the *c*- C_5H radical can be formed by substituting H in the *c*- C_3H with an ethynyl group ($-C\equiv CH$) [38].

To date, a considerable amount of theoretical and experimental effort has been made to detect more isomers of the molecular formula C_5H . Schaefer et al. theoretically studied seven isomers of C_5H and reported their optimized structures and energetics way back in 1999 [39]. In the same year, anionic and neutral forms of **1** and the branched chain isomer of C_5H , pent-1,4-diyn-1,3,5-triyl (**5**), were identified through mass spectrometry by Blanksby et al. [30]. Very recently, in 2022, isomer **2** of C_5H has been identified by Cernicharo et al. in TMC-1 using Yebes 40m radio telescope [40]. Along with the neutral molecules, several cations and anions of molecular formula C_nH have been detected in TMC-1, IRC+10216, and in other sources of ISM. In 2022, C_5H^+ and C_3H^+ were identified by the same group through the QUIJOTE line survey of TMC-1 [41].

Though isomer **3** of C_5H lies 105 kJ mol^{-1} above **1**, the net dipole moment value ($\mu = 4.73$ Debye) is quite comparable to that of isomer **1** ($\mu = 4.81$ Debye), and thus it is a potential candidate for radioastronomical studies. It is also noted here that several high-energy isomers of astronomical interest are detected not only in the laboratory but also in the ISM. For example, to date, four linear cumulene carbenes, propadienylidene (C_3H_2) [42], butatrienylidene (C_4H_2) [43], pentatetraenylidene (C_5H_2) [44–47], hexapentaenylidene (C_6H_2) [45,48], and one branched-chain cumulene carbene, ethynylbutatrienylidene (C_6H_2) [49], are identified both in the laboratory as well as in the ISM. Notably, none of these isomers are thermodynamically the most stable isomers (global minima) in their respective elemental compositions. Theoretical studies from Stanton and co-workers suggest that ethynylbutatrienylidene is 226 kJ mol^{-1} above the most stable isomer triacetylene at the CCSD(T)/cc-pVTZ level of theory [50]. From the thermodynamical perspective, though it can be considered a high-energy isomer, it was still identified both in the laboratory and in the ISM. Therefore, we rather see isomer **3** as a potential candidate, although energetically, it lies 105 kJ mol^{-1} above isomer **1**. Moreover, the abundance ratio suggested by chemical models for *c*- C_5H /*l*- C_5H is 0.069 [40]. This also indicates that cyclic isomers (both **2** and **3**) are more abundant than linear isomers for this elemental composition. Perhaps, we leave this discussion with a caveat that earlier astrochemical models did not consider isomer **3** and had only considered isomer **2** in their model calculations. It is anticipated by us that inclusion of **3** in the astrochemical model calculations may further decrease the ratio.

Considering the importance of the recent discoveries of C_5H radicals and their ionic forms in the ISM, we theoretically investigated all possible isomers of the molecular formula C_5H through high-level quantum chemical calculations. The anionic and cationic counterparts of these isomers have also been studied in both singlet and triplet ground electronic states. The spectroscopic parameters (e.g., rotational constant(s), inertial axis dipole moments along with their components, centrifugal distortion constants, etc.) have

been calculated using coupled-cluster method for all the isomers. Furthermore, thermodynamically favorable rearrangement schemes have been postulated for the formation of **1**, **2**, and **3** from high-energy isomers.

2. Computational Methodology

Several trial geometries of the molecular formula C_5H were generated from chemical intuition and using the PyAR program package [51,52]. First, the geometry optimization and frequency calculation of all the trial geometries were carried out using DFT at the UB3LYP [53,54]/6-311+G(d,p) [55,56] level of theory. Based on these geometries, further optimization calculations were carried out for all low-lying isomers and their possible cationic and anionic counterparts at the coupled-cluster singles and doubles with quasi-perturbative triple excitation (CCSD(T)) methods [57–59] using the correlation-consistent polarized valence triple zeta basis set of Dunning's (cc-pCVTZ) [60–62]. Similar to optimization, harmonic vibrational frequencies were computed at the all-electron UCCSD(T)/cc-pCVTZ level of theory. T_1 diagnostic values [63] were calculated at the UCCSD/6-311+G(d,p)//UB3LYP/6-311+G(d,p) level to assess the multireference character of all isomers.

To incorporate the empirical dispersion corrections [64], all geometry optimization and frequency calculations were also carried out at the UB3LYP-D3/6-311+G(d,p) and $U\omega B97XD$ [65]/6-311+G(d,p) level of theories. Restricted Hartree–Fock (RHF) wave function was used for singlet electronic states of anionic and cationic counterparts of all isomers, whereas, for open-shell doublet and triplet electronic states, unrestricted HF (UHF) wave function was used. All the single-step rearrangements between two isomers, through an appropriate transition state, were calculated using DFT and confirmed by intrinsic reaction coordinate (IRC) calculations at the UB3LYP/6-311+G(d,p) level of theory. All DFT calculations were performed using the Gaussian 09 suit of programs [66], and all CC calculations were carried out using the CFOUR program package [67].

3. Results and Discussion

A total of fourteen isomers, within the energy range of 0 to 312 kJ mol^{-1} from the lowest energy structure **1**, were theoretically identified on the C_5H potential energy surface (PES). The electronic structures of the first five low-lying isomers (**1**–**5**), along with their cationic and anionic forms, are shown in Figure 1. The canonical forms of isomer **1** are shown in Figure 2. The electronic structures of the rest of the isomers (**6**–**14**) are listed in Figure 3. After several attempts, structures of the isomers **13**, **14**, **3-c**, and **4-a** could not be optimized at the coupled-cluster level. Therefore, the structures of isomers **13** and **14** were presented only at the UB3LYP/6-311+G(d,p) level of theory. Also, it has been observed that isomer **14** rearranges to isomer **1** during optimization through an automatic hydrogen transfer process from C2 to C1. In a similar manner, isomer **4-a** also converts to isomer **2-a** through a ring-opening rearrangement.

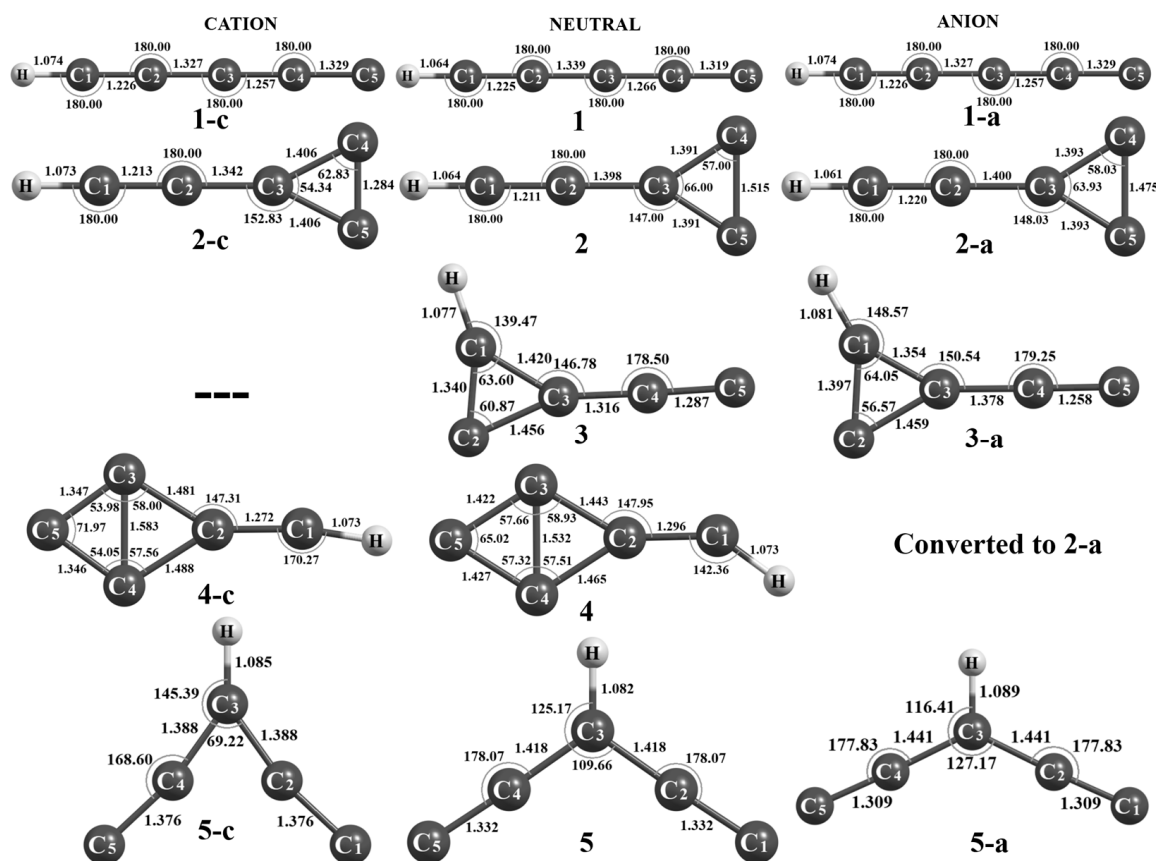


Figure 1. Optimized geometries of first five low-lying C_5H radicals along with their cationic and anionic counterparts calculated at the (U)CCSD(T)/cc-pCVTZ level of theory.

In addition, a thermodynamically favorable rearrangement scheme is postulated in Figure 4, and several appropriate transition states were also identified for the interconversion of isomers on the C_5H PES (Figures 4 and 5). The point group symmetry, zero-point vibrational energy (ZPVE) corrected relative energies (ΔE_0 ; in kJ mol^{-1}), Gibbs free energies ($\Delta G_{298.15}$; in kJ mol^{-1}), and singlet–triplet energy gaps (ΔE_{ST} ; in kJ mol^{-1}) at various levels of theory are shown in Table 1 for isomers 1–5 along with their cationic and anionic counterparts. The multireference character of these isomers was also evaluated by T_1 diagnostic values at the UCCSD/6-311+G(d,p)//UB3LYP/6-311+G(d,p) level of theory. The T_1 diagnostic is used to determine whether a single-reference-based electron correlation procedure is appropriate with self-consistent-field molecular orbitals and invariant to the same orbital rotations. If the T_1 diagnostic value is greater than 0.02, then the molecules have the multireference character. However, due to limited computational facilities, we could not perform the multireference coupled-cluster calculations for the present study. The adiabatic ionization potential ($IP = E_{Cation} - E_{neutral}$) and adiabatic electron affinity ($EA = E_{Anion} - E_{neutral}$) were calculated from their zero-point energy corrected energies of the respective cationic and anionic counterparts. Similar information for the rest of the neutral isomers is listed in Tables 2 and S13 (in the Supplementary Materials). The spectroscopic parameters, e.g., inertial axis dipole moments along with their components, rotational constants, and the centrifugal distortion constants for the first five low-lying isomers along with their cationic and anionic counterparts, are listed in Tables 3 and 4 for the rest of the neutral isomers. Final Cartesian coordinates of the optimized geometries, total energies, ZPVEs, rotational constants, singlet–triplet energy gaps, and T_1 diagnostic values are presented in the Supplementary Materials for all fourteen isomers.

Table 1. ZPVE-corrected relative energies (ΔE_0 ; in kJ mol^{-1}), Gibbs free energies ($\Delta G_{298.15}$; in kJ mol^{-1}), singlet–triplet energy gaps (ΔE_{S-T} ; in kJ mol^{-1}), T_1 diagnostic values, ionization potential (IP, in eV), electron enthalpy (EA, in eV), and $\langle S^2 \rangle$ of first five low-lying isomers along with their cations and anions of C_5H calculated at different levels.

Energy Parameter	Level of Theory	Isomer-1			Isomer-2			Isomer-3			Isomer-4			Isomer-5		
		1-c	1	1-a	2-c	2	2-a	3-c	3	3-a	4-c	4	4-a	5-c	5	5-a
ΔE_0	UCCSD(T)/cc-pCVTZ	0	0	0	105	34	−51	---	105	−76	---	160	---	369	167	188
	UB3LYP/6-311+G(d,p)	0	0	0	116	45	−13	---	105	−40	---	209	−13	377	222	−46
	UB3LYP-D3/6-311+G(d,p)	0	0	0	114	45	−12	---	104	−41	---	207	−13	375	220	−44
	U ω B97XD/6-311+G(d,p)	0	0	0	96	17	−45	−1	87	−74	---	169	---	353	194	−58
$\Delta G_{298.15}$	UCCSD(T)/cc-pCVTZ	0	0	0	102	26	−48	---	90	−70	---	168	---	359	203	138
	UB3LYP/6-311+G(d,p)	0	0	0	109	32	−16	---	92	−41	---	192	−18	365	203	−48
	U ω B97XD/6-311+G(d,p)	0	0	0	90	13	−46	3	83	−75	---	165	---	340	204	−60
	UCCSD(T)/cc-pCVTZ	262	---	−80	164	---	132	---	---	199	---	---	---	129	---	188
ΔE_{S-T}	UB3LYP/6-311+G(d,p)	136	---	−76	157	---	108	---	---	188	---	---	---	−1	---	158
	U ω B97XD/6-311+G(d,p)	121	---	−84	143	---	117	175	---	203	---	---	---	1	---	162
	UCCSD/6-311+G(d,p)//	0.022	0.040	0.024	0.027	0.024	0.027	0.051	0.049	0.018	---	0.05	0.020	0.085	0.066	0.022
T_1 Diagnostic	UB3LYP/6-311+G(d,p)	0.022	0.040	0.024	0.027	0.024	0.027	0.051	0.049	0.018	---	0.05	0.020	0.085	0.066	0.022
IP	UCCSD(T)/cc-pCVTZ	8.36	---	---	9.11	---	---	---	---	---	---	---	---	10.45	---	---
EA	UCCSD(T)/cc-pCVTZ	---	---	1.42	---	---	2.30	---	---	3.30	---	---	---	---	---	3.63
$\langle S^2 \rangle$	UCCSD(T)/cc-pCVTZ	---	0.749	---	---	0.749	---	---	0.747	---	---	0.750	---	---	0.749	---

Table 2. ZPVE-corrected relative energies (ΔE_0 ; in kJ mol^{-1}), Gibbs free energies ($\Delta G_{298.15}$; in kJ mol^{-1}), T_1 diagnostic values, and $\langle S^2 \rangle$ of isomers 6–13 of C_5H calculated at different levels.

Energy Parameter	Level of Theory	6	7	8	9	10	11	12	13
ΔE_0	UCCSD(T)/cc-pCVTZ	224	262	271	294	301	302	312	---
	UB3LYP/6-311+G(d,p)	249	260	318	320	333	336	422	428
	UB3LYP-D3/6-311+G(d,p)	248	261	319	318	332	335	422	429
	U ω B97XD/6-311+G(d,p)	214	247	277	---	299	300	380	386
$\Delta G_{298.15}$	UCCSD(T)/cc-pCVTZ	222	246	268	286	294	296	310	---
	UB3LYP/6-311+G(d,p)	228	248	304	296	318	320	405	413
	U ω B97XD/6-311+G(d,p)	203	215	267	---	293	294	373	376
	UCCSD/6-311+G(d,p)//	0.034	0.050	0.046	0.034	0.054	0.044	0.040	0.058
T_1 Diagnostic	UB3LYP/6-311+G(d,p)	0.034	0.050	0.046	0.034	0.054	0.044	0.040	0.058
$\langle S^2 \rangle$	UCCSD(T)/cc-pCVTZ	0.749	0.750	0.747	0.749	0.751	0.750	0.750	---

Table 3. Inertial axis dipole moment components, absolute dipole moments (in Debye), and centrifugal distortion constants (in MHz) and rotational constants (in MHz) of first five low-lying C₅H isomers along with their cation and anion calculated at the UCCSD(T)/cc-pCVTZ level of theory. The experimental rotational constant (in MHz) values for **1-c**, **1** and **cyclic-C₅H (2 or 3)** are listed here (from the literature). ‘s’ signifies singlet and ‘t’ signifies triplet electronic state.

Isomer	μ_a	μ_b	μ_c	$ \mu $	D_J	D_K	D_{JK}	d_1	d_2	A_e	B_e	C_e	Experiment		
													A_e	B_e	C_e
1-c-s	3.47	---	---	3.47	1.02×10^{-4}	1.02×10^{-4}	-2.05×10^{-4}	0.00	0.00	2389.14	---	---	---	2404.2	---
1-c-t	4.97	---	---	4.97	1.01×10^{-4}	1.01×10^{-4}	-2.03×10^{-4}	0.00	0.00	2331.84	---	---	---	---	---
1	4.81	---	---	4.81	1.05×10^{-4}	1.05×10^{-4}	-2.10×10^{-4}	0.00	0.00	2375.44	---	---	---	2395.127	---
1-a-s	2.98	---	---	2.98	1.01×10^{-4}	1.01×10^{-4}	-2.03×10^{-4}	0.00	0.00	2354.84	---	---	---	---	---
1-a-t	1.96	---	---	1.96	1.02×10^{-4}	1.02×10^{-4}	-2.05×10^{-4}	0.00	0.00	2352.48	---	---	---	---	---
2-c-s	2.52	---	---	2.51	2.53×10^{-4}	2.21×10^{-1}	3.22×10^{-2}	-3.01×10^{-5}	-1.82×10^{-5}	51,117.71	3511.56	3285.84	---	---	---
2-c-t	0.83	---	---	0.83	2.87×10^{-4}	2.28×10^{-1}	3.20×10^{-2}	-3.17×10^{-5}	-1.89×10^{-5}	46,241.09	3523.06	3273.65	---	---	---
2	3.26	---	---	3.26	2.88×10^{-4}	2.29×10^{-1}	3.32×10^{-2}	-3.19×10^{-5}	-1.95×10^{-5}	36,681.22	3555.18	3241.05	45,018.00	3504.06	3246.94
2-a-s	6.11	---	---	6.11	2.83×10^{-4}	2.26×10^{-1}	3.29×10^{-2}	-3.11×10^{-5}	-1.88×10^{-5}	38,715.32	3510.89	3218.98	---	---	---
2-a-t	3.59	---	---	3.59	2.69×10^{-4}	1.82×10^{-1}	2.90×10^{-2}	-2.91×10^{-5}	-1.84×10^{-5}	48,223.49	3324.13	3109.77	---	---	---
3-c-s	---	---	---	---	---	---	---	---	---	---	---	---	---	---	---
3-c-t	---	---	---	---	---	---	---	---	---	---	---	---	---	---	---
3	4.19	2.2	---	4.73	3.24×10^{-4}	1.27×10^{-1}	3.55×10^{-2}	-4.31×10^{-5}	-2.47×10^{-5}	37,025.81	3624.13	3301.02	---	---	---
3-a-s	5.15	2.75	---	5.85	2.96×10^{-4}	1.09×10^{-1}	2.70×10^{-2}	-3.51×10^{-5}	-1.96×10^{-5}	35,410.60	3605.51	3272.32	---	---	---
3-a-t	5.33	2.10	---	5.73	2.87×10^{-4}	1.08×10^{-1}	2.52×10^{-1}	-3.49×10^{-5}	-1.82×10^{-5}	36,284.2	3516.49	3205.8	---	---	---
4-c-s	---	---	---	---	---	---	---	---	---	---	---	---	---	---	---
4-c-t	5.62	0.21	---	5.62	5.22×10^{-4}	1.79×10^{-1}	9.56×10^{-3}	-8.06×10^{-5}	-1.71×10^{-5}	33,563.59	4970.89	4329.65	---	---	---
4	3.78	0.45	---	3.81	5.42×10^{-4}	1.82×10^{-1}	9.71×10^{-3}	-8.15×10^{-5}	-1.77×10^{-5}	34,960.74	4813.53	4230.99	---	---	---
4-a-s	---	---	---	---	---	---	---	---	---	---	---	---	---	---	---
4-a-t	---	---	---	---	---	---	---	---	---	---	---	---	---	---	---
5-c-s	3.48	---	---	3.48	5.70×10^{-3}	9.47×10^{-2}	-3.78×10^{-2}	-2.49×10^{-3}	-8.40×10^{-5}	12,099.53	5565.98	3812.27	---	---	---
5-c-t	2.95	---	---	2.95	5.68×10^{-3}	2.17×10^{-1}	-5.41×10^{-2}	-1.88×10^{-3}	1.49×10^{-4}	14,503.32	4145.05	3223.71	---	---	---
5	3.14	---	---	3.14	5.73×10^{-3}	2.23×10^{-1}	-5.46×10^{-2}	-1.91×10^{-3}	1.51×10^{-4}	21,155.74	3233.26	2804.62	---	---	---
5-a-s	3.5	---	---	3.5	4.48×10^{-4}	1.41×10^0	-2.96×10^{-2}	-7.57×10^{-5}	-1.74×10^{-6}	34,412.33	2686.25	2491.74	---	---	---
5-a-t	3.26	---	---	3.26	4.25×10^{-4}	1.38×10^0	-2.83×10^{-2}	-7.48×10^{-5}	-1.68×10^{-6}	37,841.38	2599.35	2432.27	---	---	---

3.1. Energetics

3.1.1. C₅H Global Minima [Pent-1,3-diyn-5-yliden-1-yl (1)]

Isomer **1** was found as the thermodynamically most stable molecule on the C₅H PES. As aforementioned, this isomer was experimentally detected in the laboratory as well as in TMC-1 [24,25]. The optimized electronic structure of **1** is linear with two acetylenic units. The ground state electronic configuration of **1** is $\dots(2\pi)^4(11\sigma)^2(3\pi)^1$. The unpaired electron at the Highest Occupied Molecular Orbital (HOMO; π) leads to the ground electronic configuration of this isomer to be $^2\Pi$. The linear isomeric form of C₅H is unusually stable because of higher resonance stabilization compared to its cyclic form. We analyzed thirteen canonical forms (as shown in Figure 2), which led to the formation of the resonance hybrid structure **1**.

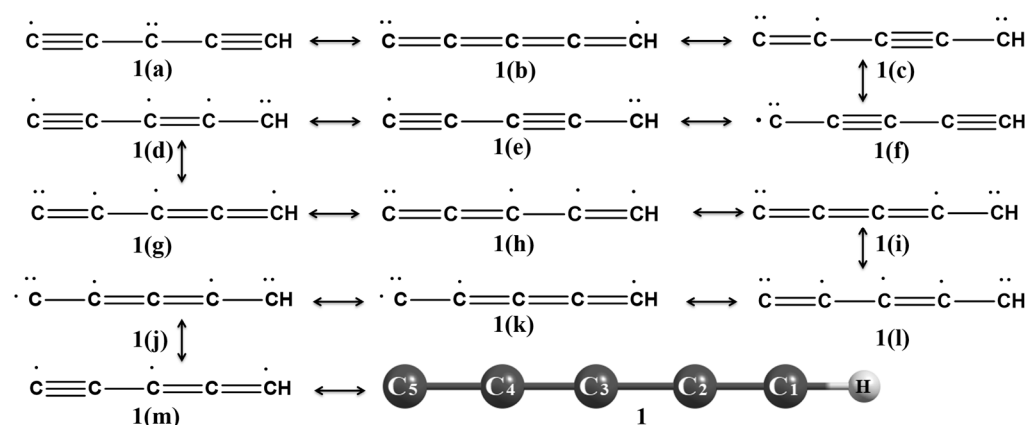


Figure 2. Possible Lewis structures (1a–1m) of **1**.

Out of all the canonical forms, the most interesting ones have either two acetylenic moieties or cumulenic bonding patterns. The valence bond structure of canonical form **1(a)**, where the carbene carbon is present at the middle carbon (C3) and two acetylenic moieties are present at the terminal position, can possibly have a bent geometry in principle. But, several trial calculations with an initial guess as a bent geometry converted to the linear structure after optimization. Moreover, the energy decreases and becomes minimum at the linear geometry during the potential energy scan of **1(a)** along the increasing bond angle of C2C3C4. Here, we note that, with one extra hydrogen atom, for C₅H₂ molecular configuration, the bent structure becomes stable with C_{2v} geometry [68–70]. For the Lewis structures with cumulenic bonding patterns, e.g., **1(c)**, **1(i)**, and **1(k)**, there are formal charge distributions between the terminal carbons (C1 and C5). This type of structure can explain the elongated triple bond for C1–C2 (1.225 Å) and C3–C4 (1.266 Å) and shortened C–C single bond for C2–C3 (1.339 Å) and C4–C5 (1.319 Å). Again, due to the required charge shift for these types of canonical forms, the overall dipole moment of **1** is relatively high (4.81 Debye), calculated at the UCCSD(T)/cc-pCVTZ level of theory.

With the addition or removal of one electron from the neutral free radical structure, we observed considerable structural changes in the anionic (C₅H[−]; **1-a**) and cationic (C₅H⁺; **1-c**) form of isomer **1**. Although the overall molecular symmetry (C_{∞v}) of the isomer remains the same for the neutral as well as the cationic and anionic counterparts, there are considerable changes in the bond distances between different carbon atoms, as shown in Figure 1. We also optimized both the singlet and triplet spin states of the closed-shell anionic and cationic forms of isomer **1**. The ground state of singlet **1-c** is $^1\Sigma^+$, with electronic configuration of $\dots(2\pi)^4(11\sigma)^2$, and the corresponding triplet state is defined as $^3\Sigma^+$ with electronic configuration $\dots(2\pi)^4(11\sigma)^1(3\pi)^1$. For the anionic form (**1-a**), the ground state of the singlet and triplet spin states are $^1\Sigma^-$ and $^3\Sigma^-$, with an electronic configuration of $\dots(2\pi)^4(11\sigma)^2(3\pi_x)^2$ and $\dots(2\pi)^4(11\sigma)^2(3\pi_x)^1(3\pi_y)^1$, respectively. From the analysis of

the frontier molecular orbital energies of both spin states, it was found that the singlet electronic state is more stable for the cationic form (**1-c**), whereas the triplet spin state is more stable for the anionic counterpart (**1-a**).

3.1.2. 1-Ethynylcycloprop-1-en-2-yl-3-ylidene (**2**) and ($2\lambda^3$ -Cycloprop-2-en-1-ylidene) ethenylidene (**3**)

Isomers **2** and **3**, abbreviated as c-C3C2H and c-C3HC2, respectively, have similar skeletal structures with one three-membered ring and an acetylenic moiety; the only difference arises due to the position of the hydrogen atom. In isomer **2**, the hydrogen atom is attached to the acetylenic moiety, whereas the hydrogen atom is attached to the three-membered ring for isomer **3**. Isomer **2** could possibly be synthesized through photodissociation or abstraction of the ring-hydrogen from one of the closely related isomeric forms of C₅H₂, ethynylcyclopropenylidene (c-C3HC2H) [71]. In a similar manner, isomer **3** could easily be formed by removing one of the ring hydrogens of 2-cyclopropen-1-ylidenethenylidene (c-C3H2C2) or removing the chain hydrogen of ethynylcyclopropenylidene (c-C3HC2H) [71]. Isomers **2** and **3** are 34 and 105 kJ mol⁻¹ higher in energy than **1** at the UCCSD(T)/cc-pCVTZ level of theory.

The ground electronic state of **2** (C_{2v} symmetric molecule) and **3** (C_s symmetric molecule) are ²B₂ and ²A', and their electronic configuration are ... (2b₁)²(10a₁)²(4b₂)¹ and ... (2a'')²(13a')²(14a')¹, respectively. Spin density distribution calculation of **2** at the UCCSD(T)/cc-pCVTZ level of theory indicates that the unpaired electron primarily exists on the C_{2v}-equivalent ring carbons, whereas, in the case of **3**, the unpaired electron is located more on the ring carbon with no hydrogen atom. From the above observations, it can be suggested that **2** is possibly the resonance hybrid of three Lewis structures, one with a delocalized three-membered ring and another two with a symmetry-breaking resonating structure with one carbene and one radical center alternating in between two ring carbons.

The C2-C3 single bond (1.398 Å) and the delocalized C3-C4 and C3-C5 bonds (1.391 Å) in isomer **2** are due to the delocalization extended from a three-membered ring to the acetylenic moiety (Figure 1). Again, the large dipole moment of **2** (3.26 Debye) is well understood using the Lewis structure arguments (canonical forms), as shown in the case of linear C₅H (**1**). In the case of **3**, the carbene center is present at the ring carbon with no hydrogen atom. Due to the absence of a hydrogen atom at the terminal carbon, the acetylenic moiety shows an allene-like character (C3-C4 = 1.316 Å and C4-C5 = 1.287 Å). Here, we note that a four-membered ring structure **15^z** (Figure 3) has an imaginary frequency (ν_i) of 175.13i cm⁻¹ and acts as the transition state for the formation of isomer **3**.

The singlet and triplet ground electronic states of the cationic counterpart of **2** (**2-c**) are ¹A₁ and ³B₂ with electronic configurations ... (2b₁)²(10a₁)² and ... (2b₁)²(10a₁)¹(4b₂)¹, respectively. The singlet–triplet energy gap (ΔE_{T-S}) was calculated as 164 kJ mol⁻¹ at the UCCSD(T)/cc-pCVTZ level of theory. The singlet ground electronic state is more stable than the triplet one. In the case of the anionic form of **2** (**2-a**), the singlet electronic state is 132 kJ mol⁻¹, more stable than the triplet electronic state. The singlet and triplet ground electronic states of **2-a** are ¹B₂ and ³A₁ with electronic configurations ... (2b₁)²(10a₁)²(4b₂)² and ... (2b₁)²(10a₁)²(4b₂)¹(11a₁)¹, respectively. The ground-state electronic structures of **2-c** (triplet) and **2-a** (singlet) are shown in Figure 1. It is evident from Figure 1 that the C1-C2 bond in each case (**2-c** = 1.213 Å, **2** = 1.211 Å, and **2-a** = 1.220 Å) act as a triple bond. Due to the presence of one unpaired electron on the C_{2v}-equivalent ring carbons, the C4-C5 bond is more like a single bond. The C₂ plane of symmetry, along with equivalent bond distances and bond angles, indicates C_{2v} symmetry.

For isomer **3**, the cationic counterpart (**3-c**) is unstable as it isomerizes to **1-c**. Thus, we are unable to optimize **3-c** (neither in singlet nor in triplet electronic state) using DFT as well as coupled-cluster methods. But, the singlet ground electronic state of the anionic counterpart (**3-a**) is more stable (ΔE_{T-S} = 199 kJ mol⁻¹) than the triplet one. The ground electronic states of singlet and triplet **3-a** are ¹A' and ³A' with electronic configuration ... (2a'')²(13a')²(14a')² and ... (2a'')²(13a')²(14a')¹(15a')¹, respectively. The closed-shell an-

ionic structure (**3-a**; as shown in Figure 1) describes shorter C1-C3 (~0.07 Å shorter than **3**) and C1-C2 (~0.06 Å shorter than **3**) bond distances compared to the neutral isomer (**3**).

3.1.3. (2λ3-Meth-1-ylidene)bicyclo[1.1.0]- But-1(3)-en-4-ylidene (**4**)

As shown in Figure 1, the optimized geometry of isomer **4** (c-C4CH) has a four-membered ring along with one CH radical attached to the C₄ ring. The ground electronic state of **4** is ²A', with electronic configuration ... (2a'')²(13a')²(14a')¹. The spin density distribution at the UCCSD(T)/cc-pCVTZ level of theory reveals that the unpaired electron is primarily present on the terminal carbon attached to the hydrogen. The skeletal C₄ ring (D_{2h} symmetric C₄ molecule) was theoretically identified by Watts et al. in 1999, which compares well with the present theoretical calculations on isomer **4** [72]. While the C_s-symmetric structure of **4** (Figure 1) with a C2C1H bond angle of 142.36° is a minimum on the C₅H PES, the C_{2v}-symmetric structure of **4** (16^z, Figure 2, 20 kJ mol⁻¹ higher energy than **4**) acts as a transition state with one imaginary frequency (426.01i cm⁻¹). The imaginary frequency corresponds to the wagging motion of the CH bond within the molecular plane, which is also confirmed by the IRC calculation at the UB3LYP/6-311+G(d,p) level (Figure S1 in Supplementary Materials).

The cationic form of isomer **4** (**4-c**) is only stable in the triplet ground electronic state (³A') with an electronic configuration of ... (2a'')²(13a')¹(14a')¹. In the optimized structure of triplet **4-c**, the C2C1H bond angle (170.27°) is ~30° higher than the neutral isomer **4**. The anionic counterpart (**4-a**) is also unstable due to the isomerization process and converts to isomer **2** by breaking one C-C bond during the optimization process.

3.1.4. Pent-1,4-diyn-1,3,5-triyl(**5**)

This isomer is symmetrically branched with the C_{2v} point group and can be abbreviated as C2CHC2. This structure is quite similar to that of ethynylpropadienylidene (C2CHC2H; C_s symmetric C₅H₂ isomer) [69,70,72]. Isomer **5** can be easily formed by removing one hydrogen atom from the ethynyl chain of C2CHC2H. The ground electronic state of **5** is ²B₁ with electronic configuration ... (8a₁)²(5b₂)²(1a₂)²(2b₁)¹. In 1999, Schaefer et al. theoretically identified isomer **5** as a C₁ symmetric molecule [39]. They showed that the geometry of **5** is far away from C_{2v} symmetry. But, according to our calculations at the UCCSD(T)/cc-pCVTZ level, one C₂ axis passes through the C3-H bond, and equivalent bond distances are measured for C2-C3 and C3-C4 (1.418 Å), as well as C1-C2 and C4-C5 (1.332 Å). Again, equivalent bond angles between C5C4C3 and C3C2C1 (178.07°) and both HCH bond angles being 125.17° prove that **5** is C_{2v} symmetric instead of C₁. All positive vibrational frequencies at the UCCSD(T)/cc-pCVTZ level indicates that isomer **5** is at a minimum on the PES.

The anionic form (**5-a**) or the cationic form (**5-c**) prepared by adding or removing one electron to isomer **5** have significant differences in the geometry, though the overall molecular symmetry (C_{2v}) remains unchanged. As shown in Figure 1, the equivalent bond distances between C2-C3 and C3-C4 decrease to 1.388 Å for **5-c**, while similar bonds increase to 1.441 Å for **5-a**. The bond angle (C4C3C2) increases with increasing electrons from **5-c** to **5-a**. For **5-c**, the C4C3C2 bond angle is 69.22°, which implies that a three-membered ring (containing C4C3C2 atoms) like skeletal is formed due to the absence of one electron. This phenomenon can be well explained by spin density calculation, and it shows that the spin density on C4 and C2 atoms is low in case **5-c**. Again, the high C4C3C2 bond angle (127.17°) of **5-a** indicates that the spin density is maximum on C4 and C2. The singlet and triplet ground electronic state of **5-c** is ¹A₂ and ³B₁ with electronic configuration ... (8a₁)²(5b₂)²(1a₂)² and ... (8a₁)²(5b₂)²(1a₂)¹(2b₁)¹, respectively. Again, in case of **5-a**, the similar configurations are ¹B₁ and ³B₂ with electronic configurations ... (8a₁)²(5b₂)²(1a₂)²(2b₁)² and ... (8a₁)²(5b₂)²(1a₂)²(2b₁)¹(5b₂)¹.

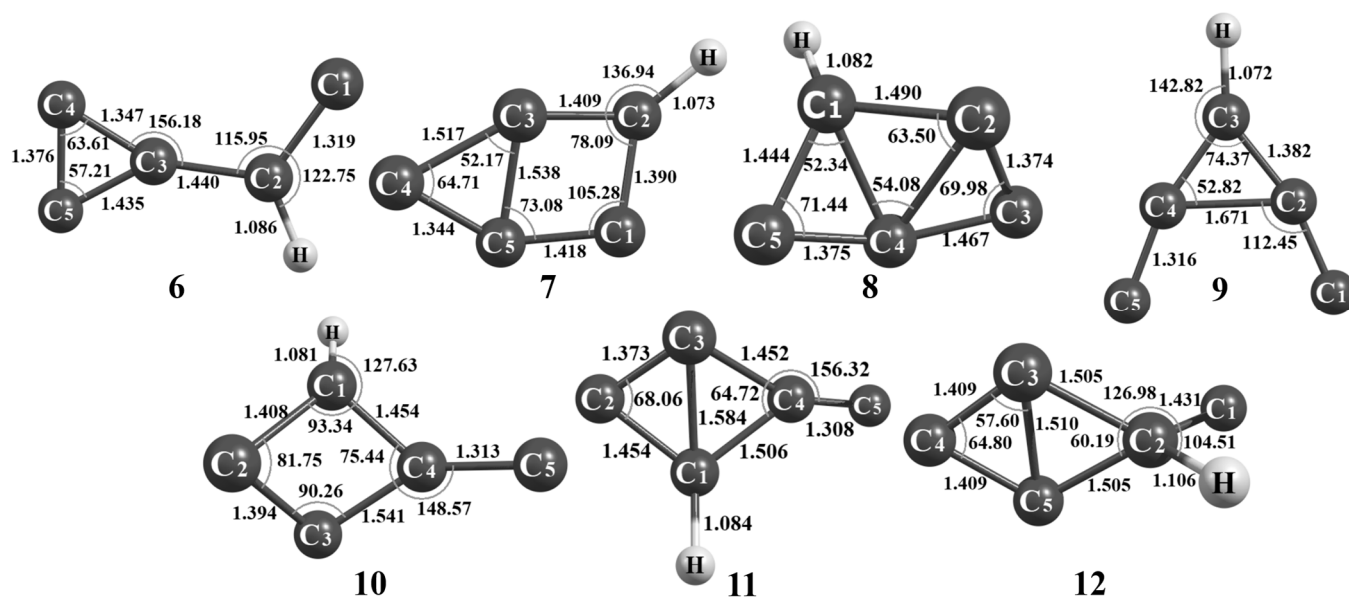


Figure 3. Optimized geometries of isomers 6 to 12 of the C₅H radicals calculated at the UCCSD(T)/cc-pCVTZ level of theory.

3.1.5. Other Isomers: C₅H (6) to C₅H (14)

Isomer 6 (abbreviated as *c*-C3CHC) is structurally similar to 2 (*c*-C3C2H), though higher in energy by 190 kJ mol⁻¹. The only difference is in the position of the hydrogen atom, which changes from the terminal carbon of the ethynyl moiety of 2 to the center carbon of 6 (Figure 3). The ground electronic state of 6 is ²A' (C_s symmetry) with electronic configuration ... (2a'')²(13a')²(14a')¹. Based on spin density distribution at the UCCSD(T)/cc-pCVTZ level, the unpaired electron primarily resides at the terminal ring carbons. Lewis structures similar to isomer 2, with a symmetry-breaking resonating structure with one carbene and one radical center alternating between two ring carbons, are also possible. The C1-C2 bond distance (1.319 Å) of the terminal ethynyl moiety is longer compared to 2, indicating its double bonding character. Thus, from the structural point of view, it is understood that the 1,2-hydrogen shifting is possible for the formation of 2 from 6 with a lower energy barrier (for detailed discussion, please refer to Section 3.2 and Figure 4).

Isomer 7 (262 kJ mol⁻¹ higher energy than 1) contains one three- and one four-membered fused ring with one hydrogen atom at C2 (Figure 3). The ground electronic state of 7 is ²A (C₁ symmetry) with electronic configuration ... (14a)²(15a)²(16a)¹. The spin density distribution at the UCCSD(T)/cc-pCVTZ level suggests that the unpaired electron primarily resides on a three-membered ring carbon atom (C4), and the C4-C5 bond distance (1.344 Å) indicates greater double bonding character. Isomer 7 is 38 kJ mol⁻¹ higher in energy than 6, and the ring-opening reactions of the strained four-membered ring can easily convert to isomer 6 with a small energy barrier.

Isomer 8 is C₁ symmetric with three three-membered fused rings. The hydrogen atom is bonded to the bridgehead position of two three-membered rings (Figure 3). The ground state of 8 is ²A, with electronic configuration is same as 7. The unpaired electrons are primarily located on the terminal carbon (C3) of the three-membered ring, where no hydrogen is attached. The coupled-cluster optimized geometry at UCCSD(T)/cc-pCVTZ level suggests that C4-C5 (1.375 Å) and C2-C3 (1.374 Å) bonds are closer to double bonding character.

The optimized geometry of isomer 9 (abbreviated as *C_c*-C3HC) is C_{2v} symmetric at the UCCSD(T)/cc-pCVTZ level with one C₂ axis passing through the central carbon atom (C3-H bond, Figure 3). The ground electronic state is ²A₂ with electronic configuration ... (8a₁)²(6b₂)²(1a₂)¹. Isomer 9 is structurally similar to that of 5, except for one C-C bond (1.671 Å) between C2 and C4. From the spin density distribution calculations, it is evident

that the unpaired electron is primarily centered on central carbon atom C3. This suggests a Lewis structure with two double bonds between C4-C5 (1.316 Å) and C2-C1 (1.316 Å). Moreover, the equivalent bond distances between C3-C4 and C3-C2 (1.382 Å) and bond angles C5C4C2 and C1C2C4 (112.45°) and C2C3H and C4C3H (142.82°) confirm that isomer **9** is a C_{2v} symmetric molecule.

Isomer **10** (c-C4HC) has one four-membered C_4 ring, a terminal carbon, and a hydrogen atom attached to the C_4 ring. The unpaired electron is primarily located on the ring carbon atom (C1 or C3) attached to the hydrogen. The optimized geometry at the UCCSD(T)/cc-pCVTZ level (Figure 3) suggests that the C2-C3 (1.394 Å) and C4-C5 (1.313 Å) bonds are more likely to be a double-bonded character. Therefore, the terminal carbon atom (C5) would act as a double-bonded carbene center. The ground electronic state of **10** is 2A with electronic configuration $\dots(14a)^2(15a)^2(16a)^1$.

Isomers **11** and **12** have structural similarities with isomer **4**, only the position of the hydrogen atom is different. While the hydrogen atom in **4** is attached to a terminal carbon atom, in the case of **11** and **12**, the hydrogen atom is attached to ring carbon atoms C1 and C4, respectively. When the position of the hydrogen atom changes from terminal carbon (C_s ; **4**) to ring carbon (C_1 ; **11** and **12**), the molecular symmetry breaks. Therefore, the ground electronic state of **11** and **12** is 2A , with the electronic configuration the same as **10**. The spin density distribution of **11** at the UCCSD(T)/cc-pCVTZ level of theory predicts that the unpaired electron is present on the C2 carbon atom. The terminal carbon acts as a double-bonded carbene center with a C4-C5 bond distance of 1.308 Å. In the case of **12**, the unpaired electron is located on the terminal carbon atom (C1). The C3-C4 (1.409 Å) and C4-C5 (1.409 Å) bonds are equal and show partial double bonding character.

Isomer **13** consists of one four-membered (C_4) ring and one bridging carbon atom. The optimization and frequency calculations were performed at the UB3LYP/6-311+G(d,p) and U ω B97XD/6-311+G(d,p) level of theories for this isomer. Due to the presence of the bridging carbon atom, the C_4 ring is no longer planar. The overall molecular symmetry of **13** is C_s , and therefore, the ground electronic state is $^2A'$, with an electronic configuration of $\dots 4(a'')^2(10a')^2(11a')^2(12a')^1$. The unpaired electron is primarily located on the C_4 ring carbon atom, the carbon attached to the hydrogen atom (C3), or on the bridgehead carbons (C2 and C4). C1-C2 and C1-C4 bond distances are more likely to be a C-C single bond with a distance of 1.555 Å. Likewise, C2-C5 and C4-C5, measuring 1.486 Å each, are also considered to be single bonds. Therefore, we can infer that C1 and C5 centers are more likely to be carbene centers.

Isomer **14** (C3CHC) is a long chain isomer with one hydrogen atom at the second carbon, which led to the zig-zag structure. The optimization and frequency calculations were carried out only at the UB3LYP/6-31+G level of theory; while optimizing at a higher level, this geometry rearranges to linear C_5H isomer (**1**) by 1,2-H shifting rearrangement.

3.2. Rearrangement Scheme

We propose several one-step thermal rearrangement schemes that led to the formation of energetically more stable isomers from the high-energy isomers of C_5H . We performed several trial calculations and identified appropriate transition states for the rearrangement processes. All the transition states and corresponding rearrangement schemes connecting the reactants and the products were verified through the intrinsic reaction coordinate (IRC) calculations at the UB3LYP/6-311+G(d,p) level of theory in Gaussian 09 software [66]. Possible rearrangement schemes studied in this work are schematically shown in Figure 4. All the transition states identified in this work are listed in Figure 6. The linear isomer (**1**) can be directly obtained through the rearrangement of isomers **2**, **3**, and **10**. Isomer **2** lies 45 kJ mol $^{-1}$ above **1**, and thus it can rearrange to **1** through the transition state TS1. A simple bond-breaking process takes place between the C3-C5 bond in the cyclopropynyl ring of **2**. The activation energy of this ring-opening reaction is 85 kJ mol $^{-1}$. TS1 has an imaginary frequency (ν_i) of 552.33i cm $^{-1}$, which corresponds to the ring-opening mechanism. The rearrangement between **3** and **1** undergoes through the ring

opening of the cyclo-propynyl ring between the C2-C3 bond and a hydrogen transfer reaction from C2 to C1, simultaneously through TS2. The activation energy of this interconversion is relatively high (131 kJ mol^{-1}) since the ring opening and the hydrogen transfer processes take place simultaneously. Here, we note that a different transition state was identified by Schaefer et al. [39], where only the ring-opening reaction takes place between C1 and C3. However, TS2 has only one imaginary frequency at $314.79i \text{ cm}^{-1}$, which corresponds to the simultaneous process of ring opening and hydrogen transfer reaction. Another direct rearrangement to the most stable isomer **1** is from **10**, which is energetically 333 kJ mol^{-1} higher than **1**. The rearrangement goes through TS3 ($\nu_i = 666.12i \text{ cm}^{-1}$) through a bond-breaking process between C1 and C4 in the four-membered ring of **10**, and the activation energy for this rearrangement is relatively less (70 kJ mol^{-1}).

Isomer **10** can also rearrange to **5** via TS4 ($\nu_i = 324.47i \text{ cm}^{-1}$), which represents the ring opening through breaking the C4-C3 bond. The activation energy of this process is merely 6 kJ mol^{-1} . Further, isomer **5** can possibly rearrange to **3** through a ring-closing reaction and 1,3-hydrogen shifting between the middle carbon atom (C3) and terminal carbon atom (C1). The transition state (TS5, $\nu_i = 646.41i \text{ cm}^{-1}$) corresponding to this simultaneous two-step isomerization process has relatively higher activation energy (153 kJ mol^{-1}). Another one-step isomerization process that led to isomer **3** is from isomer **11**. The ring-opening reaction by breaking the C3-C4 bond of **11** forms **3** through TS6 ($\nu_i = 473.06i \text{ cm}^{-1}$), which is a barrier-less process with an activation energy of $\sim 1 \text{ kJ mol}^{-1}$. This might be because of the formation of resonance-stabilized structure **3** from the strained cyclic structure of **11**.

Isomer **2** can be formed directly through rearrangement from **4** and **6**. All of the rearrangements leading to **2** have relatively less activation energy compared to the formation of isomer **1**. Isomer **4** has a fused structure of two three-membered rings, with one CH group attached to the ring carbon atom (C2). The rearrangement process between **4** and **2** undergoes through the transition state TS7 ($\nu_i = 544.24i \text{ cm}^{-1}$) through the ring-opening mechanism. The activation energy required for this rearrangement is $\sim 30 \text{ kJ mol}^{-1}$. The interconversion between **6** and **2** undergoes the hydrogen transfer reaction from C2 to C1 through the transition state TS8 ($\nu_i = 200.49i \text{ cm}^{-1}$), with the activation energy of only 2 kJ mol^{-1} . Since the activation energy for this rearrangement is very low, isomer **6** might convert to more stable isomer **2** easily. Rearrangement between **7** and **2** takes place through the formation of **6** as an intermediate via transition state TS9 ($\nu_i = 290.15i \text{ cm}^{-1}$), which represents the ring-opening mechanism of a highly strained four-membered ring. The activation energy required for this isomerization is 33 kJ mol^{-1} . Another rearrangement pathway to isomer **2** might be possible from **12**. This rearrangement may take place in two ways: first, the hydrogen shifting reaction between C2 and C1 in **12**, which leads to the formation of **4** through TS10 ($E_a = 5 \text{ kJ mol}^{-1}$, $\nu_i = 496.55i \text{ cm}^{-1}$) followed by ring opening from **4** to **2**. The second possible way is through the ring-opening reaction, first forming **6** through TS11 ($E_a = 4 \text{ kJ mol}^{-1}$, $\nu_i = 464.05i \text{ cm}^{-1}$), followed by a hydrogen shifting reaction to form **2**.

From the different rearrangement pathways discussed above, it can be inferred that the interconversion of the three lowest-energy isomers (**1**, **2**, and **3**) requires significantly higher activation energies compared to the interconversion of other high-energy isomers. However, the activation energy required for the formation of **1**, **2**, or **3** from other higher-energy isomers is comparatively less. Therefore, it can be concluded that these low-energy isomers (**1**, **2**, and **3**) will be thermodynamically and kinetically stable once formed in the laboratory or in the ISM.

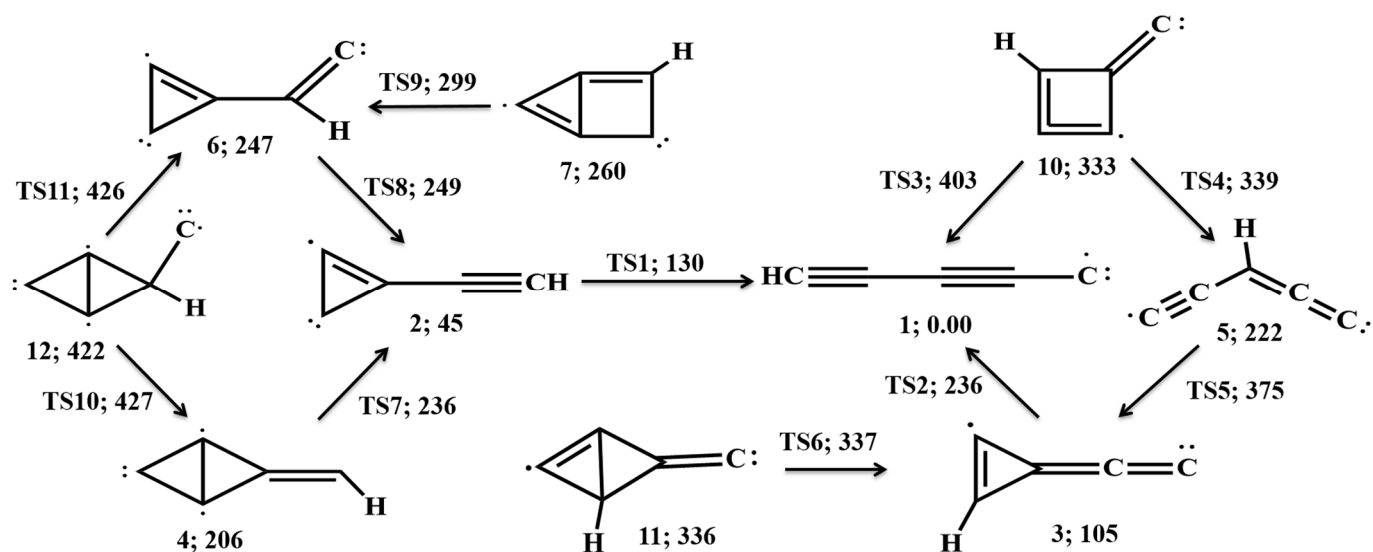


Figure 4. Rearrangement scheme for C₅H isomers to low-lying isomers calculated at UB3LYP/6-311+G(d,p) level of theory.

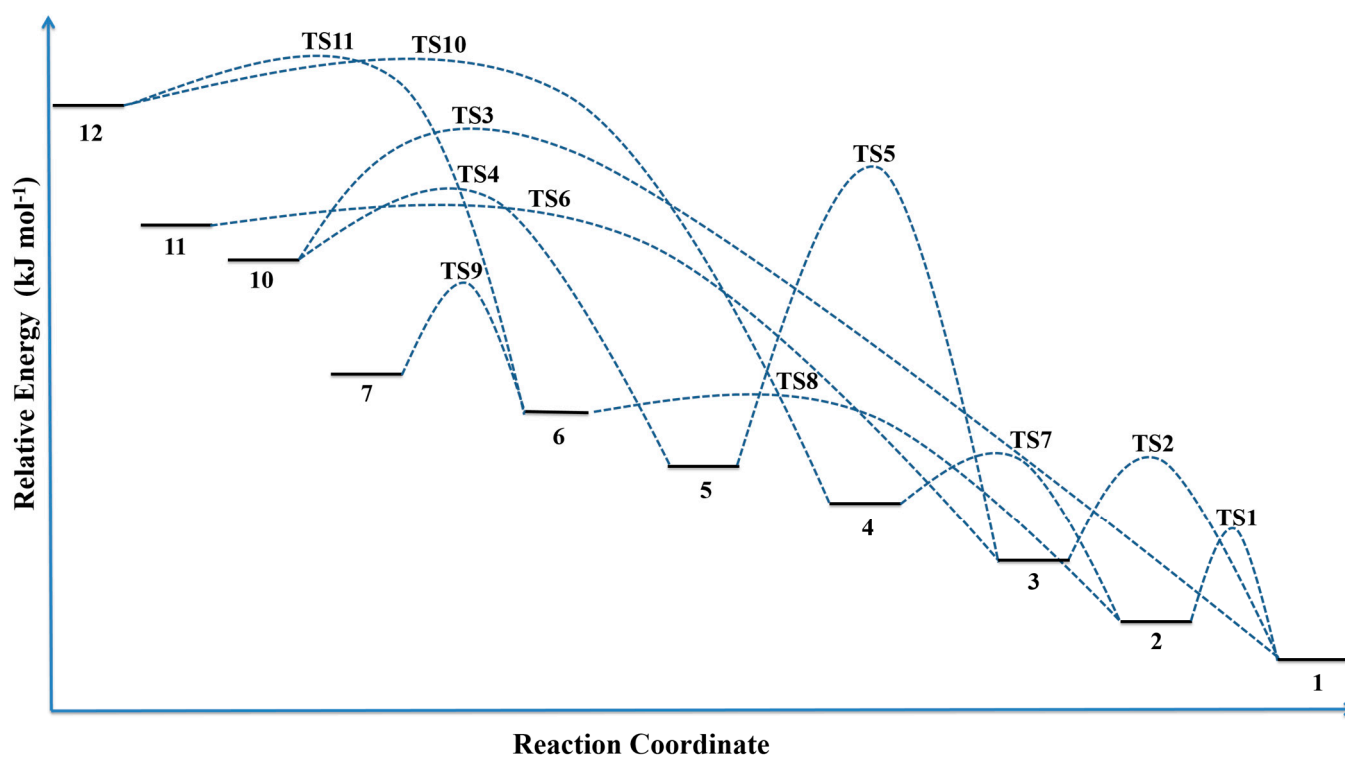


Figure 5. Potential energy surface of rearrangement scheme shown in Figure 4.

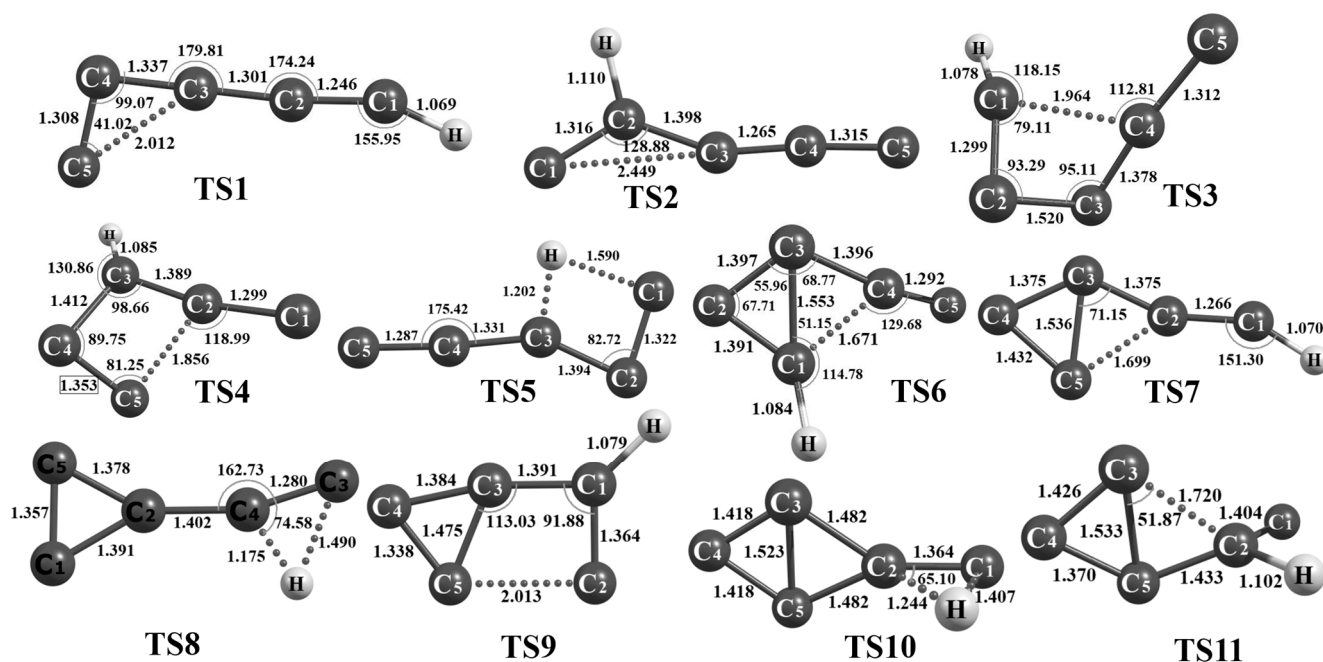


Figure 6. Optimized geometries of the transition states involved in the rearrangement scheme (shown in Figure 4) calculated at UB3LYP/6-311+G(d,p) level of theory.

3.3. Spectroscopic Data

In both the laboratory and the ISM, the spectroscopic detection of C_5H isomers has remained an open challenge for the last few decades. Therefore, the rotational constants, dipole moments, and the centrifugal distortion constant values of the first five low-lying C_5H isomers, along with their cation and anion, were calculated at the UCCSD(T)/cc-pCVTZ level of theory and are listed in Table 3. The spectroscopic detection of linear C_5H (**1**) in the laboratory was performed by Cernicharo et al. in 1986 [25] and 1987 [24], Gottlieb et al. in 1986 [36], and McCarthy et al. [37] in 1999. The experimental rotational constant for **1** is 2395.127 MHz which has a good correlation with our theoretically calculated value (2375.436 MHz) at the UCCSD(T)/cc-pCVTZ level, and the percentage error estimated is 0.83%.

The cationic form of the l - C_5H (1-c), pentadiynylidynium, is also a potential carrier for the diffused interstellar band (DIB). In 2022, Cernicharo et al. discovered the linear C_5H^+ in TMC-1 with the QUIJOTE line survey and provided a calculated rotational constant value (2404.2 MHz) and a scaled rotational constant value (2410.3 MHz) [40]. Our calculated rotational constant (2389.14 MHz) at the UCCSD(T)/cc-pCVTZ level of theory for the most stable singlet electronic state ($^1\Sigma^+$) of 1-c is in good agreement with the observed results. Here, we note that Botschwina [73] first calculated the rotational constant ($B_e = 2405 (\pm 5)$) MHz for C_5H^+ (1-c) in 1991 based on quantum chemical calculations. Later, in 2014 and 2019, Aoki [74] also obtained $B_e = \sim 2420$ MHz, and Bennedjai et al. [75] in 2019 calculated the value of B_e to be 2391.7 MHz.

The triplet ground electronic state of **1-a** ($^3\Sigma^-$) is more stable compared to $^1\Sigma^-$. Cernicharo et al. [41] provided the calculated (2366.4 MHz) and scaled (2372.4 MHz) rotational constant value for linear $^3\Sigma^-$, which compares well with our theoretical data (2352.48 MHz). Recently, Cabezas et al. discovered the cyclic C_5H radical (**2**) in TMC-1 and they provided the rotational constant values as $A_0 = 45,018(20)$ MHz, $B = 3504.0621(3)$ MHz, and $C = 3246.9414(4)$ MHz. Isomer **2** is an oblate symmetric top molecule with a high rotational constant value (A) compared to the two nearly equal rotational constants (B and C). The theoretical data at the UCCSD(T)/cc-pCVTZ level of theory predicts three rotational constants, $A_e = 36,681.219$ MHz, $B_e = 3555.179$ MHz, and $C_e = 3241.054$ MHz, which have a good agreement with the experimental data. The rotational constants, dipole moments, and centrifugal distortion constants values for isomers **2**, **3**, **4**, and **5**, along with

cationic and anionic forms in their singlet and triplet electronic state, are depicted in Table 3. Isomers 3, 4, and 5 are oblate symmetric top molecules. The spectroscopic parameters (rotational constants, dipole moments, and centrifugal distortion constants) for isomers 6 to 12 at the UCCSD(T)/cc-pCVTZ level of theory are listed in Table 4.

3.4. Ab Initio Molecular Dynamics Study

To confirm the kinetic stability of the neutral isomers of the molecular formula C_5H , the ab initio molecular dynamics simulations were performed for all fourteen isomers at 298K temperature and 1 atm pressure condition at B3LYP/6-311+G(d,p) level of theory using Gaussian 09 software. The atom-centered density matrix propagation (ADMP) is basically an extended Lagrangian molecular dynamics method that has been used to employ the atom-centered Gaussian basis functions and one-particle density matrix propagation. These simulations were executed for 10,000 fs for the first five low-lying isomers and 2500 fs for the rest of the isomers. The time evolution of the total energy of the first five minimum energy isomers (1–5) at the given condition is described in Figure 7. AIMD results for other isomers (6–14) are shown in Figure S8 (Supplementary Materials). From Figure 7, it can be clearly predicted that isomers 1, 2, and 3 are kinetically the most stable isomers. ADMP study also reveals that isomer 4 isomerizes to 2, which can be verified through the isomerization process as the activation barrier is only 36 kJ mol⁻¹. Isomer 6 converts to 3, and isomer 9 transforms to 5. Isomer 10 is kinetically unstable, and it isomerizes to 5, which can be verified from the rearrangement scheme as the activation energy for this isomerization is only 6 kJ mol⁻¹. Similarly, isomer 11 is kinetically unstable as it converts to 5.

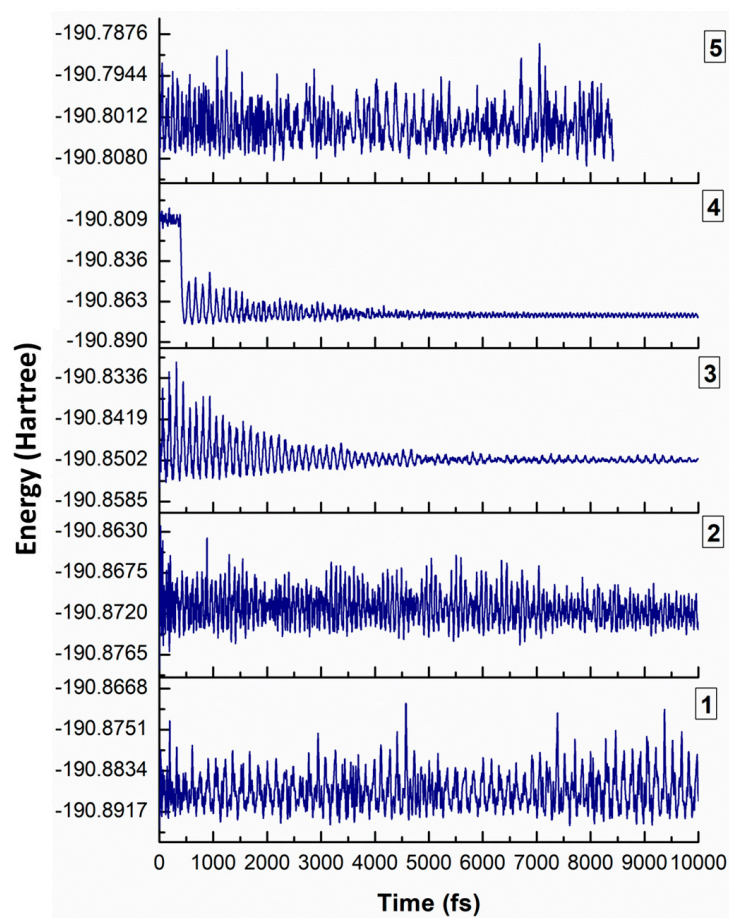


Figure 7. Energy evolution of isomer 1–5 of C_5H obtained from the AIMD simulation carried out at 298.15K temperatures and 1 atm pressure for 10,000 fs at the B3LYP/6-311+G(d,p) level of theory.

4. Conclusions

Fourteen isomers of molecular formula C_5H and their ionic counterparts were theoretically studied using DFT and coupled-cluster methods at the UB3LYP/6-311+G(d,p) and UCCSD(T)/cc-pCVTZ levels of theory. However, isomers **13** and **14** are found to convert to low-energy isomers while optimizing at the coupled-cluster level. The lowest energy isomer in its neutral radical (**1**) and cationic form (**1-c**), along with the lowest energy cyclic isomer (**2**), has recently been detected in TMC-1 and experimentally identified in the laboratory. The spectroscopic parameters computed at the UCCSD(T)/cc-pCVTZ level of theory are in good agreement with the experimental results. However, the linear C_5H^- (**1-a**) isomer has still not been detected either in the laboratory or in the ISM. This fact may be correlated to the low EA (<2 eV) obtained from the calculations. Isomer **3-a** is found to be the lowest isomer on the anionic PES, which is strongly bound (3.3 eV). It may be inferred that the addition of one electron might help to stabilize the three-membered ring of **3-a** and might be a good candidate for laboratory or astronomical detection. From the rearrangement reactions, it is evident that the first three low-lying isomers (**1**, **2**, and **3**) will be thermodynamically and kinetically stable once formed in the laboratory or in the ISM. Our current theoretical analysis indicates that isomer **3** and its ionic counterparts would be suitable candidates for detection both in the laboratory as well as in the ISM.

Supplementary Materials: The following supporting information can be downloaded at: <https://www.mdpi.com/article/10.3390/atoms11090115/s1>, Figure S1: Optimized geometries of isomers **13** to **16** of the C_5H radicals; Figure S2: Intrinsic reaction coordinate for the transition state **15^z** and **16^z** calculated at UB3LYP/6-311+G(d,p) level of theory; Figure S3: Intrinsic reaction coordinate for the rearrangement from **3** to **1** and **10** to **1** calculated at UB3LYP/6-311+G(d,p) level of theory; Figure S4: Intrinsic reaction coordinate for the rearrangement from **10** to **5** and **5** to **3** calculated at UB3LYP/6-311+G(d,p) level of theory; Figure S5: Intrinsic reaction coordinate for the rearrangement from **10** to **5** and **4** to **2** calculated at UB3LYP/6-311+G(d,p) level of theory; Figure S6: Intrinsic reaction coordinate for the rearrangement from **6** to **2** and **10** to **5** calculated at UB3LYP/6-311+G(d,p) level of theory; Figure S7: Intrinsic reaction coordinate for the rearrangement from **12** to **4** and **10** to **5** calculated at UB3LYP/6-311+G(d,p) level of theory; Figure S8: Energy evolution of isomer **6-14** of C_5H obtained from the AIMD simulation carried out at 298.15 K temperatures and 1 atm pressure for 2500 fs at the B3LYP/6-311+G(d,p) level of theory; Table S1: Optimized geometries of the C_5H isomers (**1-14**) along with their cationic and anionic forms in Cartesian coordinates (in Angstrom units) obtained at UB3LYP/6-311+G(d,p) level of theory; Table S2: Geometries of transition states involved in the rearrangement scheme in Cartesian coordinates (in Angstrom units) obtained at UB3LYP/6-311+G(d,p) level of theory; Table S3: Point group, relative zero-point corrected energy (ΔE_0 in kJ mol^{-1}), dipole moments (in Debye) and rotational constants (in MHz) of C_5H isomers of **1-14** in their ground electronic states calculated at the UB3LYP/6-311+G(d,p) level of theory; Table S4: Point group, relative zero-point corrected energy (ΔE_0 in kJ mol^{-1}), dipole moments (in Debye) and rotational constants (in MHz) of cationic counterpart of C_5H isomers of **1-14** in their singlet ground electronic states calculated at the UB3LYP/6-311+G(d,p) level of theory. Table S5: Point group, relative zero-point corrected energy (ΔE_0 in kJ mol^{-1}), dipole moments (in Debye) and rotational constants (in MHz) of anionic counterpart of C_5H isomers of **1-14** in their singlet ground electronic states calculated at the UB3LYP/6-311+G(d,p) level of theory; Table S6: Point group, relative zero-point corrected energy (ΔE_0 in kJ mol^{-1}), dipole moments (in Debye) and rotational constants (in MHz) of cationic counterpart of C_5H isomers of **1-14** in their triplet ground electronic states calculated at the UB3LYP/6-311+G(d,p) level of theory; Table S7: Point group, relative zero-point corrected energy (ΔE_0 in kJ mol^{-1}), dipole moments (in Debye) and rotational constants (in MHz) of anionic counterpart of C_5H isomers of **1-14** in their triplet ground electronic states calculated at the UB3LYP/6-311+G(d,p) level of theory; Table S8: Point group, relative zero-point corrected energy (ΔE_0 in kJ mol^{-1}), dipole moments (in Debye) and rotational constants (in MHz) of C_5H isomers of **1-14** in their ground electronic states calculated at the $U\omega B97XD/6-311+G(d,p)$ level of theory; Table S9: Point group, relative zero-point corrected energy (ΔE_0 in kJ mol^{-1}), dipole moments (in Debye) and rotational constants (in MHz) of cationic counterpart of C_5H isomers of **1-14** in their singlet ground electronic states calculated at the $U\omega B97XD/6-311+G(d,p)$ level of theory; Table S10: Point group, relative zero-point corrected energy (ΔE_0 in kJ mol^{-1}), dipole moments (in Debye) and

rotational constants (in MHz) of anionic counterpart of C₅H isomers of 1–14 in their singlet ground electronic states calculated at the U ω B97XD/6-311+G(d,p) level of theory; Table S11: Point group, relative zero-point corrected energy (ΔE_0 in kJ mol⁻¹), dipole moments (in Debye) and rotational constants (in MHz) of cationic counterpart of C₅H isomers of 1–14 in their triplet ground electronic states calculated at the U ω B97XD/6-311+G(d,p) level of theory; Table S12: Point group, relative zero-point corrected energy (ΔE_0 in kJ mol⁻¹), dipole moments (in Debye) and rotational constants (in MHz) of anionic counterpart of C₅H isomers of 1–14 in their triplet ground electronic states calculated at the U ω B97XD/6-311+G(d,p) level of theory; Table S13: Ionization potential (IP, in eV) and electron enthalpy (EA, in eV) of isomers 6 to 14 calculated at different levels of theory.

Author Contributions: Conceptualization, S.G.; methodology, A.A., V.S.T. and S.G.; software, S.S. and T.R.; validation, S.G., V.S.T. and A.A.; formal analysis, S.S. and T.R.; investigation, S.S. and T.R.; resources, S.G.; data curation, S.S. and T.R.; writing—original draft preparation, S.S., T.R. and S.G.; writing—review and editing, S.G., A.A. and V.S.T.; visualization, S.S., T.R., S.G., A.A. and V.S.T.; supervision, S.G., A.A. and V.S.T.; project administration, S.G., A.A. and V.S.T. All authors have read and agreed to the published version of the manuscript.

Funding: S.G. and A.A. thanks the Govt. of India (GoI) for grant No. DST/NSM/R&D_HPC_Applications/2021/21 for the Paramshakti HPC facilities at IIT Kharagpur. S.G. thanks for the computational facilities in NITD supported by EMR/2017/002653, and V.S.T. thanks the U.S. Department of Defense for DURIP grant W911NF-10-1-0157 and NSF CRIF grant CHE-0947087 at SDSU.

Data Availability Statement: Data are available in the article or Supplementary Materials.

Acknowledgments: SG and AA thanks the Govt. of India (GoI) for grant no DST/NSM/R&D_HPC_Applications/2021/21 for the Paramshakti HPC facilities at IIT Kharagpur and doctoral fellowship for SS. Computational facilities in NITD supported by EMR/2017/002653 and support provided at SDSU (for VST) by DURIP grant W911NF-10-1-0157 from the U.S. Department of Defense and by NSF CRIF grant CHE-0947087 are gratefully acknowledged. TR thanks NITD for the doctoral fellowship.

Conflicts of Interest: The authors declare no conflict of interest.

References

1. Adams, W.S. Some Results with the COUDÉ Spectrograph of the Mount Wilson Observatory. *Astrophys. J.* **1941**, *93*, 11. [[CrossRef](#)]
2. Dunham, T., Jr. Interstellar neutral potassium and neutral calcium. *Publ. Astron. Soc. Pac.* **1937**, *49*, 26–28. [[CrossRef](#)]
3. McKellar, A. Evidence for the Molecular Origin of Some Hitherto Unidentified Interstellar Lines. *Publ. Astron. Soc. Pac.* **1940**, *52*, 187–192. [[CrossRef](#)]
4. Swings, P.; Rosenfeld, L. Considerations regarding interstellar molecules. *Astrophys. J.* **1937**, *86*, 483–486. [[CrossRef](#)]
5. Endres, C.P.; Schlemmer, S.; Schilke, P.; Stutzki, J.; Müller, H.S. The cologne database for molecular spectroscopy, CDMS, in the virtual atomic and molecular data centre, VAMDC. *J. Mol. Spectrosc.* **2016**, *327*, 95–104. [[CrossRef](#)]
6. Müller, H.S.; Schlöder, F.; Stutzki, J.; Winnewisser, G. The Cologne Database for Molecular Spectroscopy, CDMS: A useful tool for astronomers and spectroscopists. *J. Mol. Struct.* **2005**, *742*, 215–227. [[CrossRef](#)]
7. Müller, H.S.; Thorwirth, S.; Roth, D.; Winnewisser, G. The Cologne database for molecular spectroscopy, CDMS. *Astron. Astrophys.* **2001**, *370*, L49–L52. [[CrossRef](#)]
8. McGuire, B.A. 2021 Census of Interstellar, Circumstellar, Extragalactic, Protoplanetary Disk, and Exoplanetary Molecules. *Astrophys. J. Suppl. Ser.* **2022**, *259*, 30. [[CrossRef](#)]
9. Mebel, A.M.; Kim, G.-S.; Kislov, V.V.; Kaiser, R.I. The reaction of tricarbon with acetylene: An ab initio/RRKM study of the potential energy surface and product branching ratios. *J. Phys. Chem. A* **2007**, *111*, 6704–6712. [[CrossRef](#)]
10. Roy, T.; Ghosal, S.; Thimmakondur, V.S. Six Low-Lying Isomers of C₁₁H₈ Are Unidentified in the Laboratory—A Theoretical Study. *J. Phys. Chem. A* **2021**, *125*, 4352–4364. [[CrossRef](#)]
11. Roy, T.; Satpati, S.; Thimmakondur, V.S.; Ghosal, S. Theoretical Investigation on C₁₁H₈ Bicyclic Carbene and Allene Isomers. *Front. Phys.* **2022**, *10*, 907466. [[CrossRef](#)]
12. Roy, T.; Thimmakondur, V.S.; Ghosal, S. New Carbenes and Cyclic Allenes Energetically Comparable to Experimentally Known 1-Azulenylcarbene. *ACS Omega* **2022**, *7*, 30149–30160. [[CrossRef](#)]
13. Schmidt, T.; Boguslavskiy, A.; Pino, T.; Ding, H.; Maier, J. Optical detection of C₉H₃, C₁₁H₃, and C₁₃H₃ from a hydrocarbon discharge source. *Int. J. Mass Spectrom.* **2003**, *228*, 647–654. [[CrossRef](#)]
14. McGuire, B.A. 2018 Census of Interstellar, Circumstellar, Extragalactic, Protoplanetary Disk, and Exoplanetary Molecules. *Astrophys. J. Suppl. Ser.* **2018**, *239*, 17. [[CrossRef](#)]
15. Woon, D.E. A correlated ab initio study of linear carbon-chain radicals C_nH (n = 2–7). *Chem. Phys. Lett.* **1995**, *244*, 45–52. [[CrossRef](#)]

16. Irvine, W.; Hoglund, B.; Friberg, P.; Askne, J.; Ellder, J. The increasing chemical complexity of the Taurus dark clouds—Detection of CH₃CCH and C₄H. *Astrophys. J.* **1981**, *248*, L113–L117. [[CrossRef](#)]
17. Nyman, L.-A. Detection of CS and C₂H in absorption. *Astron. Astrophys.* **1984**, *141*, 323–327.
18. Pardo, J.R.; Cernicharo, J. Molecular Abundances in CRL 618. *Astrophys. J.* **2007**, *654*, 978–987. [[CrossRef](#)]
19. Teyssier, D.; Fossé, D.; Gerin, M.; Pety, J.; Abergel, A.; Roueff, E. Carbon budget and carbon chemistry in Photon Dominated Regions. *Astron. Astrophys.* **2004**, *417*, 135–149. [[CrossRef](#)]
20. Thaddeus, P.; Gottlieb, C.; Hjalmarsen, A.; Johansson, L.; Irvine, W.; Friberg, P.; Linke, R. Astronomical identification of the C₃H radical. *Astrophys. J.* **1985**, *294*, L49–L53. [[CrossRef](#)]
21. Tucker, K.; Kutner, M.; Thaddeus, P. The ethynyl radical C₂H—A new interstellar molecule. *Astrophys. J.* **1974**, *193*, L115–L119. [[CrossRef](#)]
22. Turner, B.E.; Herbst, E.; Terzieva, R. The Physics and Chemistry of Small Translucent Molecular Clouds. XIII. The Basic Hydrocarbon Chemistry. *Astrophys. J. Suppl. Ser.* **2000**, *126*, 427–460. [[CrossRef](#)]
23. Bell, M.; Feldman, P.; Watson, J.; McCarthy, M.; Travers, M.; Gottlieb, C.; Thaddeus, P. Observations of long C_nH molecules in the dust cloud TMC-1. *Astrophys. J.* **1999**, *518*, 740. [[CrossRef](#)]
24. Cernicharo, J.; Guélin, M.; Walmsley, C. Detection of the hyperfine structure of the C₅H radical. *Astron. Astrophys.* **1987**, *172*, L5.
25. Cernicharo, J.; Kahane, C.; Gomez-Gonzalez, J.; Guélin, M. Tentative detection of the C₅H radical. *Astron. Astrophys.* **1986**, *164*, L1–L4.
26. Cernicharo, J.; Kahane, C.; Gomez-Gonzalez, J.; Guélin, M. Detection of the ²Pi_{3/2} state of C₅H. *Astron. Astrophys.* **1986**, *167*, L5–L7.
27. Guélin, M.; Cernicharo, J.; Travers, M.; McCarthy, M.; Gottlieb, C.; Thaddeus, P.; Ohishi, M.; Saito, S.; Yamamoto, S. Detection of a new linear carbon chain radical: C₇H. *Astron. Astrophys.* **1997**, *317*, L1–L4.
28. Saito, S.; Kawaguchi, K.; Suzuki, H.; Ohishi, M.; Kaifu, N.; Ishikawa, S.-I. Detection of C₆H in the ²Pi_{1/2} state toward IRC+ 10216. *Publ. Astron. Soc. Jpn.* **1987**, *39*, 193–199.
29. Suzuki, H.; Ohishi, M.; Kaifu, N.; Ishikawa, S.-I.; Kasuga, T. Detection of the interstellar C₆H radical. *Publ. Astron. Soc. Jpn.* **1986**, *38*, 911–917.
30. Blanksby, S.J.; Dua, S.; Bowie, J.H. Generation of Two Isomers of C₅H from the Corresponding Anions. A Theoretically Motivated Mass Spectrometric Study. *J. Phys. Chem. A* **1999**, *103*, 5161–5170. [[CrossRef](#)]
31. Fossé, D.; Cernicharo, J.; Gerin, M.; Cox, P. Molecular carbon chains and rings in TMC-1. *Astrophys. J.* **2001**, *552*, 168. [[CrossRef](#)]
32. Gottlieb, C.A.; Vrtilek, J.; Gottlieb, E.; Thaddeus, P.; Hjalmarsen, A. Laboratory detection of the C₃H radical. *Astrophys. J.* **1985**, *294*, L55–L58. [[CrossRef](#)]
33. Liszt, H.; Pety, J.; Gerin, M.; Lucas, R. HCO, c-C₃H and CF⁺: Three new molecules in diffuse, translucent and “spiral-arm” clouds. *Astron. Astrophys.* **2014**, *564*, A64. [[CrossRef](#)]
34. McGuire, B.A.; Carroll, P.B.; Loomis, R.A.; Blake, G.A.; Hollis, J.M.; Lovas, F.J.; Jewell, P.R.; Remijan, A.J. A Search for l-C₃H⁺ and l-C₃H in Sgr B₂ (N), Sgr B₂ (OH), and the Dark Cloud TMC-1. *Astrophys. J.* **2013**, *774*, 56. [[CrossRef](#)]
35. Yamamoto, S.; Saito, S.; Ohishi, M.; Suzuki, H.; Ishikawa, S.-I.; Kaifu, N.; Murakami, A. Laboratory and Astronomical Detection of the Cyclic H₃H Radical. *Astrophys. J.* **1987**, *322*, L55. [[CrossRef](#)]
36. Gottlieb, C.; Gottlieb, E.W.; Thaddeus, P. Laboratory detection of the C₅H radical. *Astron. Astrophys.* **1986**, *164*, L5.
37. McCarthy, M.; Chen, W.; Apponi, A.; Gottlieb, C.; Thaddeus, P. Hyperfine Structure of the C₅H, C₆H, and C₈H Radicals. *Astrophys. J.* **1999**, *520*, 158. [[CrossRef](#)]
38. Apponi, A.; Sanz, M.; Gottlieb, C.; McCarthy, M.; Thaddeus, P. The cyclic C₅H radical. *Astrophys. J.* **2001**, *547*, L65. [[CrossRef](#)]
39. Crawford, T.D.; Stanton, J.F.; Saeh, J.C.; Schaefer, H.F. Structure and energetics of isomers of the interstellar molecule C₅H. *J. Am. Chem. Soc.* **1999**, *121*, 1902–1911. [[CrossRef](#)]
40. Cabezas, C.; Agúndez, M.; Fuentetaja, R.; Endo, Y.; Marcelino, N.; Tercero, B.; Pardo, J.R.; de Vicente, P.; Cernicharo, J. Discovery of the cyclic C₅H radical in TMC-1. *Astron. Astrophys.* **2022**, *663*, L2. [[CrossRef](#)]
41. Cernicharo, J.; Agúndez, M.; Cabezas, C.; Fuentetaja, R.; Tercero, B.; Marcelino, N.; Endo, Y.; Pardo, J.; de Vicente, P. Discovery of C₅H⁺ and detection of C₃H⁺ in TMC-1 with the QUIJOTE line survey. *Astron. Astrophys.* **2022**, *657*, L16. [[CrossRef](#)]
42. Cernicharo, J.; Gottlieb, C.; Guélin, M.; Killian, T.; Paubert, G.; Thaddeus, P.; Vrtilek, J. Astronomical detection of H₂CCC. *Astrophys. J.* **1991**, *368*, L39–L41. [[CrossRef](#)]
43. Cernicharo, J.; Gottlieb, C.; Guélin, M.; Killian, T.; Thaddeus, P.; Vrtilek, J. Astronomical detection of H₂CCCC. *Astrophys. J.* **1991**, *368*, L43–L45. [[CrossRef](#)]
44. Cabezas, C.; Tercero, B.; Agúndez, M.; Marcelino, N.; Pardo, J.; de Vicente, P.; Cernicharo, J. Cumulene carbenes in TMC-1: Astronomical discovery of l-H₂C₅. *Astron. Astrophys.* **2021**, *650*, L9. [[CrossRef](#)]
45. McCarthy, M.; Travers, M.; Kovács, A.; Chen, W.; Novick, S.E.; Gottlieb, C.; Thaddeus, P. Detection and characterization of the cumulene carbenes H₂C₅ and H₂C₆. *Science* **1997**, *275*, 518–520. [[CrossRef](#)] [[PubMed](#)]
46. Steglich, M.; Fulara, J.; Maity, S.; Nagy, A.; Maier, J.P. Electronic spectra of linear HC₅H and cumulene carbene H₂C₅. *J. Chem. Phys.* **2015**, *142*, 244311. [[CrossRef](#)]
47. Blanksby, S.J.; Dua, S.; Bowie, J.H.; Schröder, D.; Schwarz, H. Gas-phase syntheses of three isomeric C₅H₂ radical anions and their elusive neutrals. a joint experimental and theoretical study. *J. Phys. Chem. A* **1998**, *102*, 9949–9956. [[CrossRef](#)]

48. Langer, W.; Velusamy, T.; Kuiper, T.; Peng, R.; McCarthy, M.; Travers, M.; Kovacs, A.; Gottlieb, C.; Thaddeus, P. First astronomical detection of the cumulene carbon chain molecule H_2C_6 in TMC-1. *Astrophys. J.* **1997**, *480*, L63. [[CrossRef](#)]
49. McCarthy, M.C.; Thaddeus, P. Laboratory Detection of a Bent-Chain Carbene Isomer of C_6H_2 . *Astrophys. J.* **2002**, *569*, L55. [[CrossRef](#)]
50. Sattelmeyer, K.W.; Stanton, J.F. Computational studies of C_6H_2 isomers. *J. Am. Chem. Soc.* **2000**, *122*, 8220–8227. [[CrossRef](#)]
51. Nandi, S.; McAnanama-Brereton, S.R.; Waller, M.P.; Anoop, A. A tabu-search based strategy for modeling molecular aggregates and binary reactions. *Comput. Theor. Chem.* **2017**, *1111*, 69–81. [[CrossRef](#)]
52. Khatun, M.; Majumdar, R.S.; Anoop, A. A Global Optimizer for Nanoclusters. *Front. Chem.* **2019**, *7*, 644. [[CrossRef](#)] [[PubMed](#)]
53. Lee, C.; Yang, W.; Parr, R.G. Development of the Colle-Salvetti correlation-energy formula into a functional of the electron density. *Phys. Rev. B* **1988**, *37*, 785. [[CrossRef](#)]
54. Becke, A.D. Density-functional exchange-energy approximation with correct asymptotic behavior. *Phys. Rev. A* **1988**, *38*, 3098. [[CrossRef](#)]
55. Krishnan, R.; Binkley, J.S.; Seeger, R.; Pople, J.A. Self-consistent molecular orbital methods. XX. A basis set for correlated wave functions. *J. Chem. Phys.* **1980**, *72*, 650–654. [[CrossRef](#)]
56. Clark, T.; Chandrasekhar, J.; Spitznagel, G.W.; Schleyer, P.V.R. Efficient diffuse function-augmented basis sets for anion calculations. III. The 3-21+ G basis set for first-row elements, Li–F. *J. Comput. Chem.* **1983**, *4*, 294–301. [[CrossRef](#)]
57. Bartlett, R.J.; Purvis, G.D. Many-body perturbation theory, coupled-pair many-electron theory, and the importance of quadruple excitations for the correlation problem. *Int. J. Quantum Chem.* **1978**, *14*, 561–581. [[CrossRef](#)]
58. Pople, J.; Krishnan, R.; Schlegel, H.; Binkley, J. Electron correlation theories and their application to the study of simple reaction potential surfaces. *Int. J. Quantum Chem.* **1978**, *14*, 545–560. [[CrossRef](#)]
59. Raghavachari, K.; Trucks, G.W.; Pople, J.A.; Head-Gordon, M. A fifth-order perturbation comparison of electron correlation theories. *Chem. Phys. Lett.* **1989**, *157*, 479–483. [[CrossRef](#)]
60. Peterson, K.A.; Dunning, T.H., Jr. Accurate correlation consistent basis sets for molecular core–valence correlation effects: The second row atoms Al–Ar, and the first row atoms B–Ne revisited. *J. Chem. Phys.* **2002**, *117*, 10548–10560. [[CrossRef](#)]
61. Kendall, R.A.; Dunning, T.H., Jr.; Harrison, R.J. Electron affinities of the first-row atoms revisited. Systematic basis sets and wave functions. *J. Chem. Phys.* **1992**, *96*, 6796–6806. [[CrossRef](#)]
62. Woon, D.E.; Dunning, T.H., Jr. Gaussian basis sets for use in correlated molecular calculations. V. Core-valence basis sets for boron through neon. *J. Chem. Phys.* **1995**, *103*, 4572–4585. [[CrossRef](#)]
63. Lee, T.J.; Taylor, P.R. A diagnostic for determining the quality of single-reference electron correlation methods. *Int. J. Quantum Chem.* **1989**, *36*, 199–207. [[CrossRef](#)]
64. Grimme, S.; Antony, J.; Ehrlich, S.; Krieg, H. A consistent and accurate ab initio parametrization of density functional dispersion correction (DFT-D) for the 94 elements H–Pu. *J. Chem. Phys.* **2010**, *132*, 154104. [[CrossRef](#)]
65. Chai, J.-D.; Head-Gordon, M. Long-range corrected hybrid density functionals with damped atom–atom dispersion corrections. *Phys. Chem. Chem. Phys.* **2008**, *10*, 6615–6620. [[CrossRef](#)]
66. Frisch, M.J.; Trucks, G.W.; Schlegel, H.B.; Scuseria, G.E.; Robb, M.A.; Cheeseman, J.R.; Scalmani, G.; Barone, V.; Petersson, G.A.; Nakatsuji, H.; et al. *Gaussian 09, Revision D.01*; Gaussian, Inc.: Wallingford, CT, USA, 2013.
67. Matthews, D.A.; Cheng, L.; Harding, M.E.; Lipparini, F.; Stopkiewicz, S.; Jagau, T.-C.; Szalay, P.G.; Gauss, J.; Stanton, J.F. Coupled-cluster techniques for computational chemistry: The CFOUR program package. *J. Chem. Phys.* **2020**, *152*, 214108. [[CrossRef](#)]
68. Thimmakonda, V.S.; Karton, A. The quest for the carbene bent-pentadiynylidene isomer of C_5H_2 . *Chem. Phys.* **2018**, *515*, 411–417. [[CrossRef](#)]
69. Thimmakonda, V.S.; Ulusoy, I.; Wilson, A.K.; Karton, A. Theoretical studies of two key low-lying carbenes of C_5H_2 missing in the laboratory. *J. Phys. Chem. A* **2019**, *123*, 6618–6627. [[CrossRef](#)]
70. Karton, A.; Thimmakonda, V.S. From molecules with a planar tetracoordinate carbon to an astronomically known C_5H_2 carbene. *J. Phys. Chem. A* **2022**, *126*, 2561–2568. [[CrossRef](#)]
71. Seburg, R.A.; McMahon, R.J.; Stanton, J.F.; Gauss, J. Structures and stabilities of C_5H_2 isomers: Quantum chemical studies. *J. Am. Chem. Soc.* **1997**, *119*, 10838–10845. [[CrossRef](#)]
72. Watts, J.D.; Gauss, J.; Stanton, J.F.; Bartlett, R.J. Linear and cyclic isomers of C_4 . A theoretical study with coupled-cluster methods and large basis sets. *J. Chem. Phys.* **1992**, *97*, 8372–8381. [[CrossRef](#)]
73. Botschwina, P. Ab initio calculations on HC^+_5 , a cation of interest to astrochemistry. *J. Chem. Phys.* **1991**, *95*, 4360–4365. [[CrossRef](#)]
74. Aoki, K. Rotational constants of linear and/or bent C_{n+1}H^+ and C_nN^+ ($n = 1-6$): A DFT study. *Adv. Space Res.* **2014**, *54*, 1651–1658. [[CrossRef](#)]
75. Bennedjai, S.; Hammoutène, D.; Senent, M.L. Theoretical Characterization of C_3H and C_5H and Their Anions. *Astrophys. J.* **2019**, *871*, 255. [[CrossRef](#)]

Disclaimer/Publisher’s Note: The statements, opinions and data contained in all publications are solely those of the individual author(s) and contributor(s) and not of MDPI and/or the editor(s). MDPI and/or the editor(s) disclaim responsibility for any injury to people or property resulting from any ideas, methods, instructions or products referred to in the content.